Energy Conversion and Management 196 (2019) 1080–1088

Contents lists available at ScienceDirect

Energy Conversion and Management

journal homepage: www.elsevier.com/locate/enconman

Rapid microwave-assisted biomass delignification and lignin depolymerization in deep eutectic solvents

Pranjali D. Muley[a,*], Justin K. Mobley[b], Xinjie Tong[c], Brian Novak[c], Joseph Stevens[d], Dorel Moldovan[c], Jian Shi[d], Dorin Boldor[a,*]

[a] Department of Biological and Agricultural Engineering, Louisiana State University and Agricultural Center, Baton Rouge, LA 70803, United States
[b] Department of Chemistry, University of Kentucky, Lexington, KY 40546, United States
[c] Department of Mechanical and Industrial Engineering, Louisiana State University, Baton Rouge, LA 70803, United States
[d] Department of Biosystems and Agricultural Engineering, University of Kentucky, Lexington, KY 40546, United States

ARTICLE INFO

Keywords:
Deep eutectic solvents
Lignin depolymerization
Biomass deconstruction
Microwave heating

ABSTRACT

Biomass deconstruction and lignin depolymerization was performed using three different deep eutectic solvents. Various temperature (110°, 130°, and 150 °C) and time (1, 5, 10, 15 min) conditions were tested in a 2450 MHz microwave reactor. Oxalic acid (130 °C, 15 min) and formic acid DES (150 °C, 15 min) gave the highest lignin yield. Microwave heating reduced the processing time significantly. NMR characterization shows that microwave heating promotes selective bond cleavage during lignin depolymerization and has a narrow molecular weight distribution compared to conventional heating techniques. Molecular dynamic simulations showed that certain lignin bonds are stretched under the electric field imparted during microwave irradiation, increasing its probability of breaking.

1. Introduction

Pretreatment of lignocellulosic biomass is a critical step in biofuel production, lignin is being generated as a byproduct of biomass pretreatment [1,2]. Despite its great potential to produce a wide range of chemicals, lignin remains severely underutilized [2]. It is critical to convert lignin waste streams to high value-added chemicals for the economic viability and success of a bio-refinery, enabling cost-competitive biofuel and chemical production [3–5].

The heterogeneity of lignin (both in its varied bond chemistry and its variability between plants), is the primary hurdle to its targeted upgrading and reuse as a feedstock for chemicals and advanced materials. Lignin is a complex hetero-biopolymer composed primarily of three different monomers (monolignols; H, G and S,) connected through as many as eight different bonding motifs. The most common bonding motif is the β-O-4 linkage [6,7]. During lignin extraction and depolymerization processes, lignin polymers are prone to multiple chemical modifications, resulting in a heterogeneous mixture from which it is difficult to analyze and separate individual lignols [3,8,9]. Thus, the key to lignin valorization is selective depolymerization of lignin and recovery of the end-products.

Existing techniques for biomass deconstruction and lignin depolymerization such as mechanical comminution [10], thermochemical processing, steam explosion, ammonia fiber explosion, acid or alkali hydrolysis, and organosolvation methods have limitations related to efficiency and scalability [11]. Ionic liquids (ILs) have received increasing interest because of their high efficacy in fractionating biomass and decreasing the recalcitrance [12,13]. However, certain ionic liquids are expensive and environmentally toxic, inhibit enzyme activity, and often require extensive postprocessing in the form of water washes to remove residual IL [14]. The recent discovery of the deep eutectic solvent (DES) provided a new technique for biomass fractionation and lignin extraction application. DES is a mixture of two or more chemicals acting as either hydrogen-bond donors (HBD) or hydrogen-bond acceptors (HBA) [15]. DES is intrinsically cheaper than many ILs due to low precursor cost, simple synthesis and recyclability [16]; meanwhile DES can selectively dissolve lignin from plant materials [17]. DES's are shown to selectively dissolve lignin from biomass through mild acid-base catalysis mechanism [11,18]. While there are various combinations of hydrogen bond acceptor and donor (HBA and HBD) that could form deep eutectic solvents, only a few have found to be effective in delignification of biomass. A combination of oxalic acid – choline chloride, formic acid – choline chloride and lactic acid – choline chloride have shown to effectively dissolve lignin during biomass pretreatment [19–21]. Moreover, the ratio of HBD to HBA also plays and important role during biomass fractionation [21–22]. Recent studies

* Corresponding authors.
E-mail addresses: pmuley1@lsu.edu (P.D. Muley), dboldor@agcenter.lsu.edu (D. Boldor).

https://doi.org/10.1016/j.enconman.2019.06.070
Received 23 April 2019; Received in revised form 24 June 2019; Accepted 25 June 2019

have showed that DES can effectively cause cleavage of primary linkage between xylan and lignin, thus selectively separating lignin fraction from lignocellulosic biomass [11,15,23–24]. These results are highly encouraging in terms of using DES's for lignin preprocessing and depolymerization. However, mechanism of lignin deconstruction using DES has not been fully explored. Understanding this mechanism can help us tune the reaction by selecting suitable HBD and HBA to generate a low molecular weight lignin product [11]. Existing biomass fractionation and lignin depolymerization methods using DES are time intensive with reaction times of about 2–16 h [11,24].

Microwave heating has been widely applied in organic chemistry as microwaves are known to accelerate reactions, decrease reaction time and increase product selectivity [25–28] Despite a few studies reported using microwave heating for biomass pretreatment, application of microwave heating towards lignin fractionation and depolymerization using electrolytic solvents has been limited [29]. Combination of DES and microwave heating for biomass deconstruction was reported by Liu and coworkers [23]. They showed a significant decrease in time required for biomass deconstruction using microwave irradiation. They also noted that the use of microwaves led to cleavage of bonds between xylan and lignin, resulting in higher lignin extraction with microwave heating than conventional heating. The above-mentioned studies show encouraging results in the use of microwaves and electrolytic solvents for biomass deconstruction. However, we did not come across any studies targeting lignin degradation using DES and microwaves.

We hypothesize that the combination of microwave heating and electrolytic solvents can selectively depolymerize lignin with higher efficiency than that of current processes. In this study we test different types of DES for biomass fractionation as well as lignin depolymerization. Various time–temperature combinations are investigated in a microwave digestor for their ability to tune the reaction to provide control for targeted bond scission during lignin depolymerization. We also performed molecular dynamics (MD) simulations to investigate the effect of microwave heating on bond energies. MD simulation was performed on three lignin G tetramers in a deep eutectic solvent (DES) composed of choline chloride and oxalic acid (1:1 ratio) with and without a microwave field. Since the lignin force field used in our simulations is of non-reactive type we could not directly investigate the potential breaking of bonds. However, the MD simulations allowed us to investigate how the transfer of the microwave energy to kinetic and internal (e.g., inter-atomic bond stretching) energies of the molecules affects the dynamical and structural characteristics, such as bond length distributions, of the system.

2. Materials and methods

Pinewood sawdust was milled to sizes < 250 μm and dried in a convection oven for 24 h at 103 °C. Oxalic acid, lactic acid, formic acid, choline chloride, kraft lignin, and sulfuric acid were obtained from Sigma Aldrich (St. Louis, MO, USA).

2.1. DES preparation

DES were prepared in a 2450 MHz batch microwave (Milestones Inc. Shelton, CT, USA). The binary mixtures of molar ratio of 1:1 for oxalic acid-choline chloride and lactic acid-choline chloride and 2:1 for formic acid-choline chloride were heated in a batch microwave reactor. Choline chloride and oxalic acid were dried in a desiccator prior to mixing. The mixtures were heated for 60 s until a transparent liquid was obtained. The liquid was cooled to room temperature.

2.2. Dielectric measurements

Dielectric properties of deep eutectic solvents were determined using an Agilent ENA series E5071C Network Analyzer and Agilent 85070E dielectric probe kit (Agilent Technologies, Inc. Santa Carla, CA) using a slim form open-ended probe method in a 201-point frequency sweep from 280 to 4500 MHz. The network analyzer was controlled by Agilent 85070E dielectric kit software (Agilent Technologies, Inc. Santa Carla, CA) and calibrated using the 3-point method (short-circuit, air and water at 25 °C).

2.3. Biomass deconstruction

5% of dried and milled biomass was mixed with 30 g DES. This ratio was chosen based on previously reported studies. [20,30–31] The mixture was then heated in a fully instrumented and controlled Ethos X batch microwave system (Milestones Inc.Shelton, CT, USA), having a maximum power output of 1.6 kW operating at a frequency of 2450 MHz. The microwave system consisted of Teflon® sample holders of 100 mL capacity with magnetic stirrers to ensure constant mixing of the biomass and DES mixture. The sample holders were rotating about a central axis of a carousel which minimized temperature inhomogeneity. The microwave is equipped with a fiber optic temperature sensor for accurate temperature control. The heating ramp-up time was 5 min with a chamber vent time of 10 min. The DES + biomass mixtures were heated at 3 different temperatures (110, 130 and 150 °C) at 4 residence times (1-, 5-, 10-, and 15-min.) under a maximum pressure of 10 bar.

2.4. Regeneration and purification

For regeneration of dissolved lignin, the resulting liquid mixture of DES/wood was poured in a 250 mL breaker containing 15 mL anhydrous ethanol. The beaker was sealed with parafilm and the mixture was stirred for 15 min. The solid residue which mainly consists of cellulose rich residue (CRR) was separated through filtration using a ceramic funnel fitted with 20 μm filter paper on a Buchner flask under vacuum. CRR was washed with pure ethanol five times to dissolve any residual DES followed by multiple DI water washings to remove any excess ethanol and DES. The CRR was dried in a desiccator overnight and the weight was noted. To regenerate dissolved lignin, 100 mL of DI water (anti-solvent) was added to the filtrate and stirred for 1 hr. The addition of anti-solvent resulted in precipitation of lignin which was then vacuum filtered using a 0.8 μm filter paper on a Buchner flask. This step was repeated until no lignin precipitation occurred. Lignin residue on the filter paper was washed five times with 9:1 water–-ethanol solvent. The residue was dried in the desiccator, weighed and sampled. The used DES was purified using rotovap. Cellulose rich matter and lignin yields were quantified. Samples with highest lignin yield were further characterized.

2.5. Lignin depolymerization

Commercially available kraft lignin was depolymerized using deep eutectic solvents in the same microwave reactor. The depolymerization was carried out using oxalic acid-choline chloride DES at 130 °C for 15 min and formic acid- choline chloride DES at 150 °C for 15 min. Biomass deconstruction and lignin depolymerization were carried out in a conventional oil bath for comparison with microwave heating. The time and temperature combination resulting in the highest lignin yield in the microwave reactor was selected for comparison.

2.6. Characterization

The weight-average molecular weight (M_w) and number-average molecular weight (M_n) of lignin following reactions were determined by GPC. The lignin was acetylated via acetobromination [32]. Molecular weight distribution of products after the reaction were analyzed by direct injection into an HPLC system equipped with a Mixed-D PLgel column (5 μm particle size, 300 × 7.5 mm i.d., molecular weight range of 200 – 400,000 μm, Polymer Laboratories, Amherst, MA, USA) at 50 °C·THF was flowed at 0.5 mL-min-1 for 30 min. The elution profile of

the column was measured by UV absorbance at 280 nm and calibrated using a polystyrene standards kit (Sigma-Aldrich, St. Louis, MO). Chemical structures of alkaline lignin and treated lignin were determined using a Thermo Nicolet 870 FTIR-ATR spectrometer. Lignin sample spectra were obtained with 64 scans at wavelengths from 700 to 4000 cm^{-1} with a spectral resolution of 1.928 cm^{-1}. The raw FTIR spectra were baseline corrected and normalized using Omnic 6.1a software and compared in the range 750–4000 cm^{-1}. ^{1}H–^{13}C-HSQC NMR was performed on a JEOL ECZr 500 MHz Spectrometer (JEOL USA Inc., Peabody, MA) using the pulse sequence 'hsqc_dec_club_pn'. All samples were dissolved (100 mg) in 4:1 DMSO-d_6: Pyridine-d_5. Ultrasonication and autogenous heat from the sonication bath was used to increase the lignin solubility. The spectral widths were set to 220 ppm and 15 ppm for ^{13}C and ^{1}H, respectively. In all cases, the number of scans was set to 48, with a 1.5 s acquisition delay and 256 increments in F1. MestReNova 12.0 was used for spectrum processing. Apodization was used with a 90° sine bell in f2 and a 90° squared sine bell with 0.5 as the first point in f1.

2.7. MD simulations

All simulations were performed with the GROMACS 2018.1 package [33]. The interactions of particles were described by the all atom CHARMM36 force field [34]. Force field parameters and topology files for choline and oxalic acid were generated from SwissParam [35]. Lignin tetramer models and topologies were created via LigninBuilder [36]. The systems were composed of 500 choline ions, 500 chloride ions, 500 oxalic acid molecules, and one lignin G tetramer. Initial configurations were built using PACKMOL [37]. A simulation system is shown in Fig. 1. Bond constraints were applied only to bonds involving hydrogens using LINCS [38] and a 1.8 fs time step was used so that we could obtain carbon–oxygen and carbon–carbon bond length distributions. The cutoff for Van der Waals and short-range Coulomb interactions was 1.2 nm. A switching function was applied to the Van der Waals potential to change it smoothly zero between 1.0 and 1.2 nm. Particle mesh Ewald (PME) [39] was used for long range Coulomb interactions with a Fourier spacing of 0.12 and an order of four. The thermostat of Bussi, Donadio, and Parrinello [40] was used only on solvent molecules to maintain the temperature at 423.15 K. Periodic boundary conditions were applied in all directions. The microwave electric field strength was E = 0.1 V/nm and the frequency 2.45 GHz. For reference and comparison we also investigated the behavior of pure DES systems in the presence of microwave field of different strengths (E = 0.0, 0.05, 0.075, and 0.1 V/nm). These results are presented in the Supplemental Information file. Due to the high viscosity of the DES, an annealing procedure was applied to speed up equilibration. The temperature was first set at 600 K and linearly cooled down to 423.15 K over 10 ns at a constant pressure of 1 bar. Then the temperature was held at 423.15 K for another 20 ns for further equilibration and to obtain the average volume. This provided the starting configuration for simulations of another 300 ns at 423.15 K and constant volume with or without electric field. The first 20 ns of these final simulations with electric field were discarded.

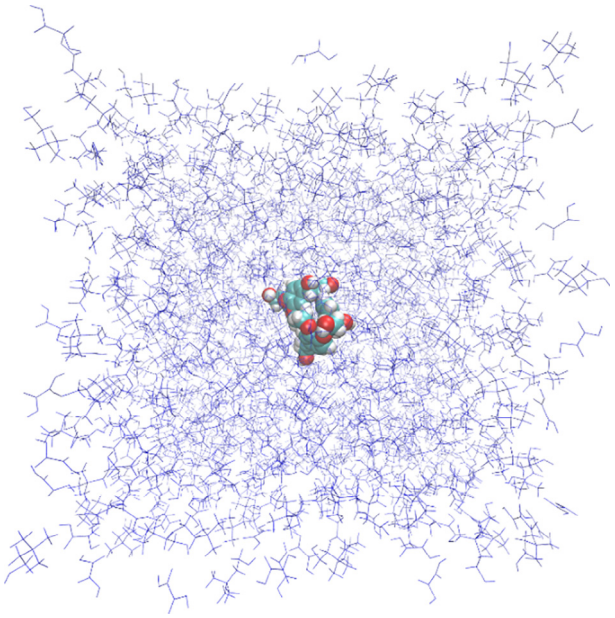

Fig. 1. A simulation box containing one (β-O-4, β-O-4, β-O-4) G tetramer (spheres) and DES solvent molecules (purple lines).

3. Results and discussion

3.1. Dielectric properties of deep eutectic solvents

Microwave heating is governed by dielectric properties of the material [41]. To understand the microwave-material interaction of deep eutectic solvents, we measured the dielectric properties of all three DESs at different frequencies. Fig. 2 shows the dielectric constant and loss values for lactic acid, oxalic acid, and formic acid DES with choline chloride. As the frequency increased, both dielectric loss and constant values decreased.

Lactic acid DES had the lowest dielectric constant values at all frequencies followed by oxalic acid and formic acid DES. At 2450 MHz, the dielectric constant value for formic acid is noted as 18.0 while that for oxalic acid and lactic acid the values are 15.0 and 10.0 respectively. Dielectric constant attributes to the ability of the material to store electrical energy in an electric field. Thus, for deep eutectic solvents heated using microwave energy, the dielectric permittivity or constant is a relative measure of its polarity. Since dipole polarization dictates microwave heating of polar molecules, higher dielectric constant values are desired for efficient dielectric heating [41]. Dielectric loss values quantify the dissipation of electromagnetic energy of dielectric material to heat energy. The dielectric loss values also followed a similar trend with loss values of 16.2, 8.1, and 5.05 at 2450 MHz for formic acid, oxalic acid, and lactic acid DES.

3.2. Biomass deconstruction using DES in microwave reactor

We studied deconstruction of biomass to obtain cellulose rich matter and lignin. Fig. 3 shows % lignin recovered after microwave assisted processing using three different DESs at various time and temperatures. For all three DESs, the lowest lignin recovery was observed at 110 °C. As the temperature increased, lignin recovery increased, except for when oxalic acid was applied at 150 °C for 15 min. This could be because at higher temperatures lignin tends to agglomerate, and filtered with CRM which could reduce lignin recovery during purification step. Lignin recovery also increased as the residence time inside the microwave increased. Among the three DESs, lactic acid DES recovered the least amount of lignin while formic acid DES had the highest recovery. At 150 °C, formic acid DES showed consistent lignin recovery at all residence times. Thus 150 °C and 1 to 15 min of processing time with formic acid and 130 °C with 15 min with oxalic acid can be considered optimum time–temperature combination. This time–temperature combination was also used for the lignin depolymerization reaction.

The extracted lignin from biomass fractionation and depolymerized kraft lignin was further analyzed. Table 1 shows the GPC data for treated lignin at various conditions [MW- and CH-represents microwave treated and conventionally treated kraft lignin (KL) or PL (pinewood lignin), respectively]. Due to the macropolymeric structure of lignin, the molecular weight of kraft lignin in its native form is high. The average molecular weight (M_w) for native lignin varies from 9000 to 13000 Da [24,42]. During processing of pure kraft lignin using DES, the

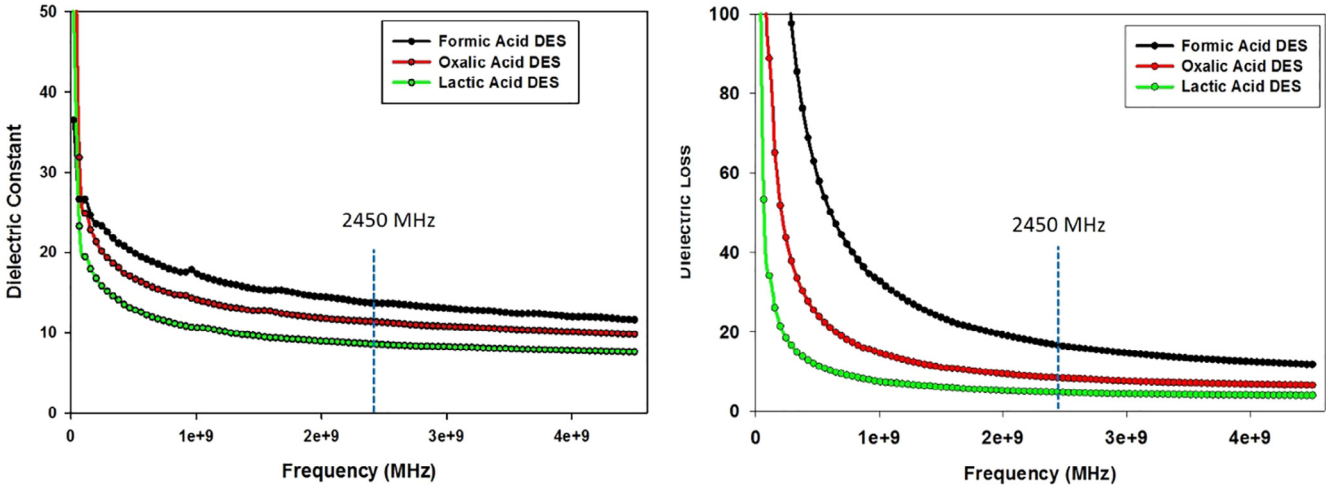

Fig. 2. Dielectric properties of three DES mixtures at varying frequencies.

average molecular weight (M_w) of lignin decreased with both types of DESs. Similarly, the type of processing also affected the molecular weight of processed lignin. For instance, the M_w of microwave treated kraft lignin was lower than with the conventional heating method at all processing parameters. For formic acid DES, the M_w of microwave treated lignin was 3538 Da while that for oxalic acid DES was 5345 Da, indicating a higher degree of depolymerization with formic acid DES treatment of lignin.

Similarly, lignin recovered from pretreated biomass also showed depolymerization. Lower M_w was observed for microwave treated biomass (2375 Da and 5691 Da for oxalic acid and formic acid DES) compared to conventional treatment (9038 Da and 7357 Da). This could be attributed to the fact that microwave heating provides direct volumetric heating and because DES molecules also move in sync with the electric field in the microwave system, it may help in breaking these bonds [20,23]. Since both DES and lignin are microwave absorbent, the degree of depolymerization is higher for microwave treated samples. In order to obtain a similar degree of depolymerization using conventional oil bath reactor, the residence time required is on the order of 2–6 h [11,24]. The polydispersity index (PDI) for both DES was lower for microwave treated lignin compared to conventional treatment, for all samples except oxalic-PL, indicating more narrow molecular weight

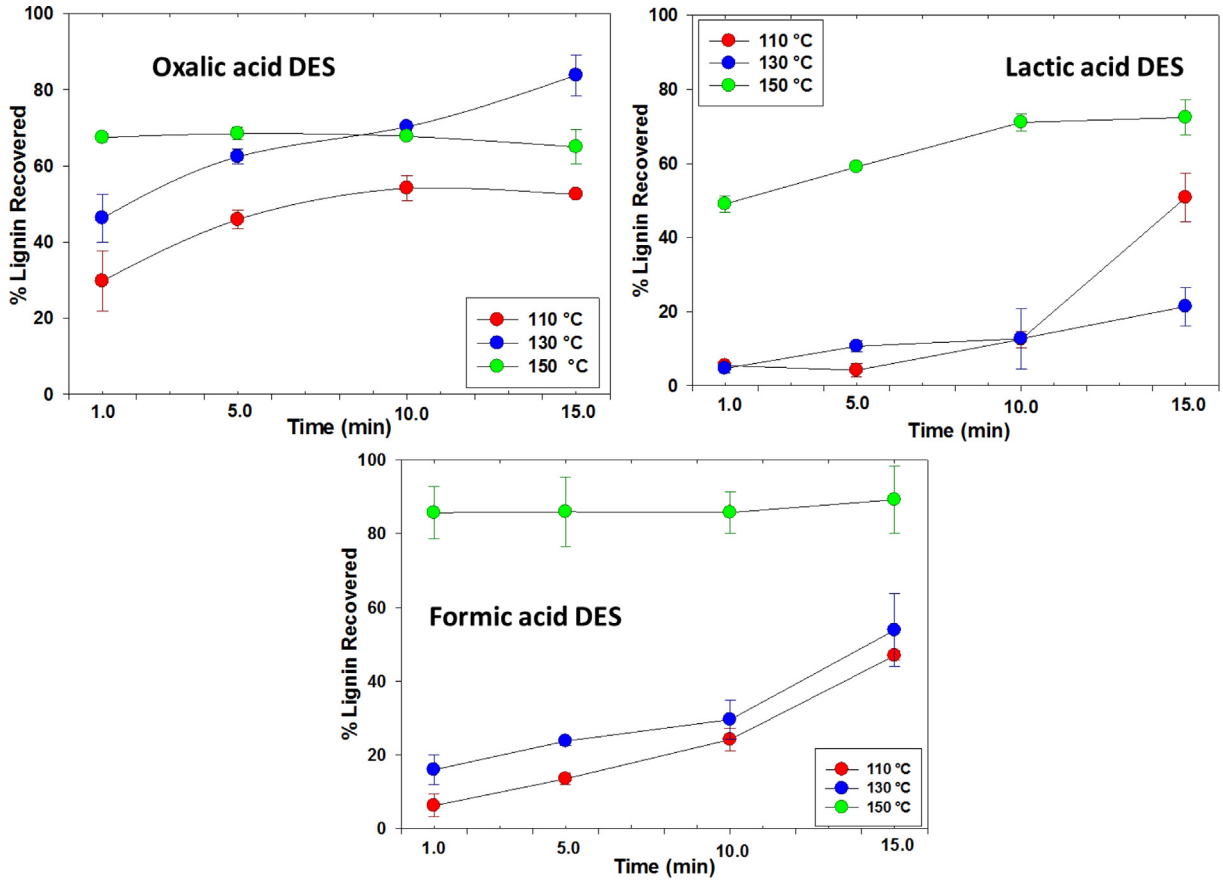

Fig. 3. Percent lignin recovery values for biomass treated with (a) oxalic acid DES, (b) lactic acid DES, and; (c) formic acid DES.

Table 1
GPC analysis of lignin showing average molecular weights (Da) and polydispersity (M_w/M_n) index of treated and untreated lignin.

Sample	M_w	M_n	PDI
Oxalic-MW-KL	5345	1951	2.73
Oxalic-CH-KL	5475	558	9.80
Formic-MW-KL	3538	509	6.94
Formic-CH-KL	9243	823	11.22
Oxalic-MW-PL	2373	208	11.41
Oxalic-CH-PL	9038	1647	5.48
Formic-MW-PL	5691	1647	3.45
Formic-CH-PL	7357	1095	6.71
Kraft Lignin [24]	9544	1915	4.89

distribution in microwave treated lignin [24,43]. These results confirm that the DES tested are effective solvents for biomass pretreatment and lignin depolymerization in a microwave environment. It should also be noted that while hemicellulose was not analyzed, deep eutectic solvents have also found to dissolve hemicellulose to some extent. Hemicellulose was either partially dissolved in the DES and was not precipitated and the remaining could remain in the cellulose rich matter [19,44].

Fig. 4 shows FTIR spectra of native lignin and lignin precipitated from DES treatment of kraft lignin. Peaks at 3388 cm^{-1} corresponds to hydroxyl groups (O–H) from aliphatic and aromatic compounds. This peak is reduced for DES treated lignin for all samples with intensity being lower for microwave heated lignin compared to conventional heating. The decrease in intensity indicates that both hydroxyl groups decreased for pretreated lignin samples [45]. The C–H bond in methyl and methylene groups is represented by twin peaks labelled as peak 2. This peak remained unchanged for conventional heating but decreased for microwave treatment indicating weakening of C–H bond during microwave processing. A carbonyl peak is observed at 1670 cm^{-1} corresponding to stretching of C = O functional group representing the lignin side chain conjugated with aromatic compounds (peak 4) [24,45]. This peak is similar both treated and untreated lignin. A peak for aromatic skeletal vibration and ring stretching was observed at 1592 and 1511 cm^{-1} (peaks 5 & 6) [24]. Similarly, peak 7 and 8 indicate the C–H deformation which decreased in the treated lignin. The intensity of these peaks indicate that the aromatic nature of lignin is intact post treatment. The intensity was significantly lower for peak 6 and non-existent for peak 8 for microwave treated lignin which could be attributed to formation of oxidized lignin subunits during microwave treatment. The peak at 1368 cm^{-1} represents the phenolic hydroxyl group [46]. The intensity of this peak is higher in treated lignin compared to untreated lignin. This could be attributed to the cleavage of β-O-4 bonds during pretreatment. This effect is also reflected through the decrease in intensity of the peak at 1130 cm^{-1}. [46] The peaks at 1267 and 856 (peak 9 & 13) corresponds to guaiacyl units. Peak 10 at 1219 cm^{-1} corresponds to guaicayl rings and a decrease in the intensity of this peak for microwave treated lignin indicates that microwave treatment reduces the G unit content during depolymerization of lignin. Similarly, peak 12 which is a C-O-C stretching at 1033 cm^{-1} decreased for microwave pretreated lignin [43,45]. These results indicate that microwave treatment is more efficient for lignin depolymerization compared to conventional heating methods.

Lignin obtained from biomass deconstruction of pine wood sawdust also showed signs of depolymerization. Fig. 5 shows IR spectra of lignin obtained after biomass deconstruction using DES through microwave and conventional heating. Peak 1 disappeared while peak 2 decreased in intensity for microwave processed sawdust, indicating hydroxyl groups decreased and C–H bonds in methyl and methylene groups weakened for both DES types. Peaks 5–7 remained intact for both conventional and microwave treated samples, indicating that no change in aromatic compounds for lignin was detected. Peak 8 intensity was reduced for microwave assisted pretreatment confirming the presence of oxidized lignin subunits. These observations confirm partial depolymerization of lignin during biomass deconstruction [24].

To understand the nature of depolymerized lignin, we identified the structures using 2D HSQC NMR spectroscopy. Kraft lignin (KL) was used as a control and NMR analysis was conducted on KL and KL treated with DES in microwave and conventional process (KL-MW, KL-CH). The cross peaks detected in the side chain region of the HSQC spectra of pure kraft lignin at δ_C/δ_H 71/4.9 (A_α), 84/4.4 (A_β) and 61/3.5 (A_γ) confirmed the presence of *β-O-4* substructure (Fig. 6, blue markup) [47]. However, the *β-O-4* linkages disappeared for all other samples treated with DES. The cross-signal of the methoxyl group was

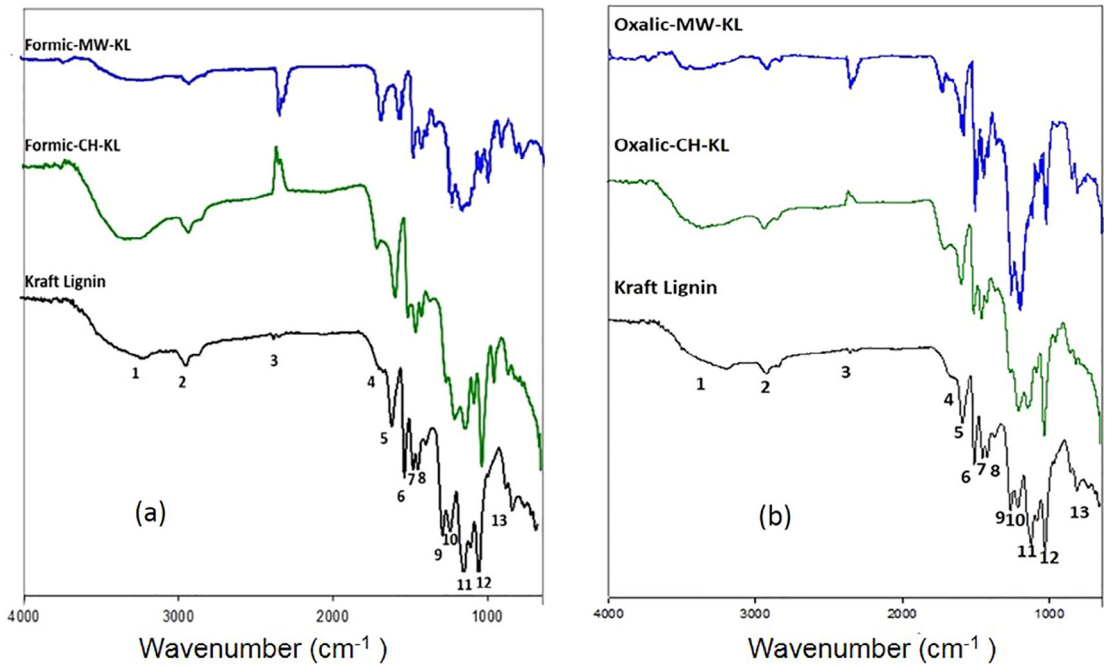

Fig. 4. FT-IR analysis of native KL and KL treated with (a) formic acid-choline chloride DES and (b) oxalic acid – choline chloride DES with microwave and conventional set heating.

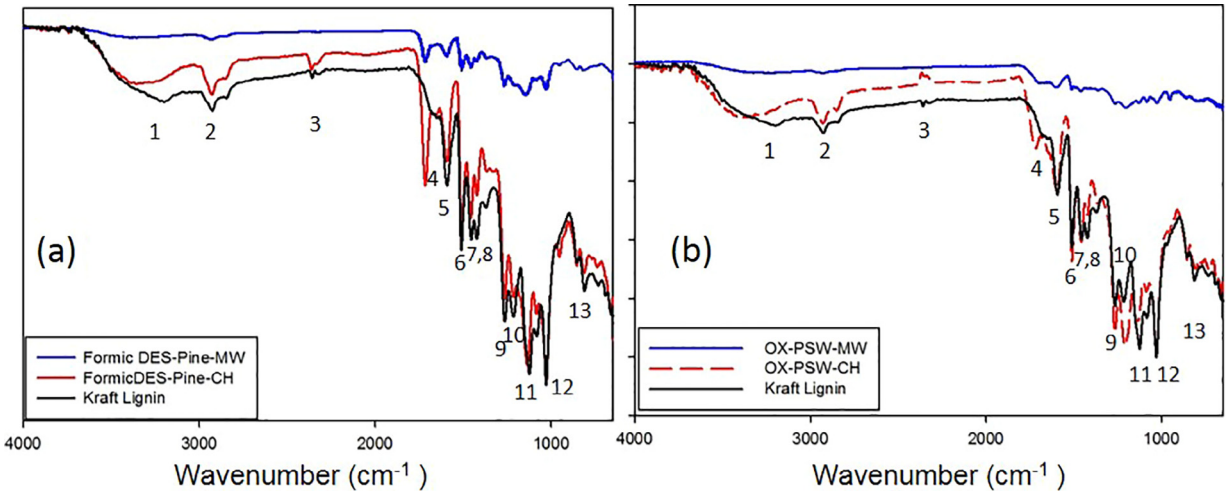

Fig. 5. FT-IR analysis of lignin extracted from pinewood treated with (a) formic acid – choline chloride DES and (b) oxalic acid-choline chloride DES in microwave and conventional set up.

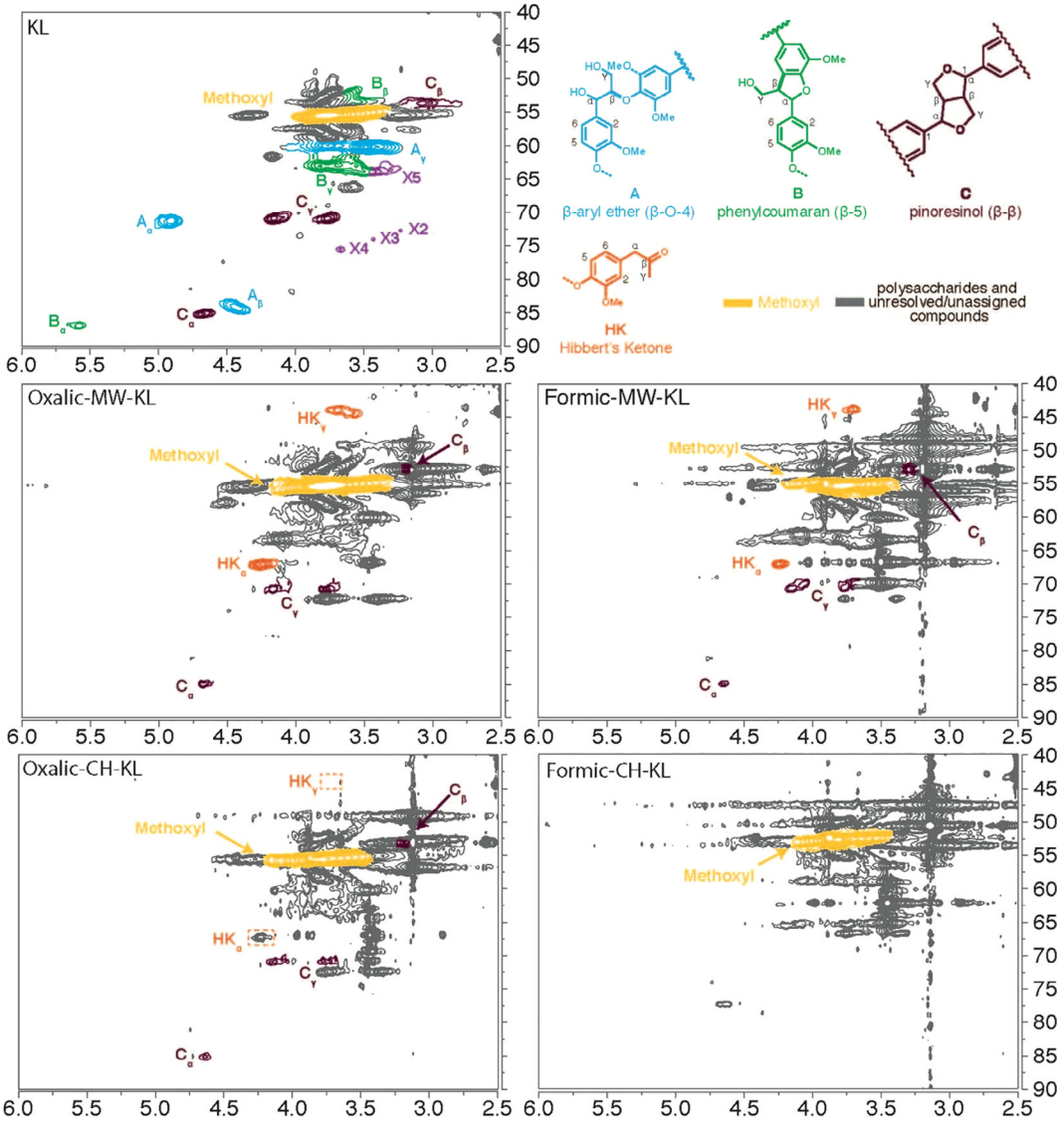

Fig. 6. HSQC NMR spectra of the aliphatic region of kraft lignin before and after MW and CH treatment in DES.

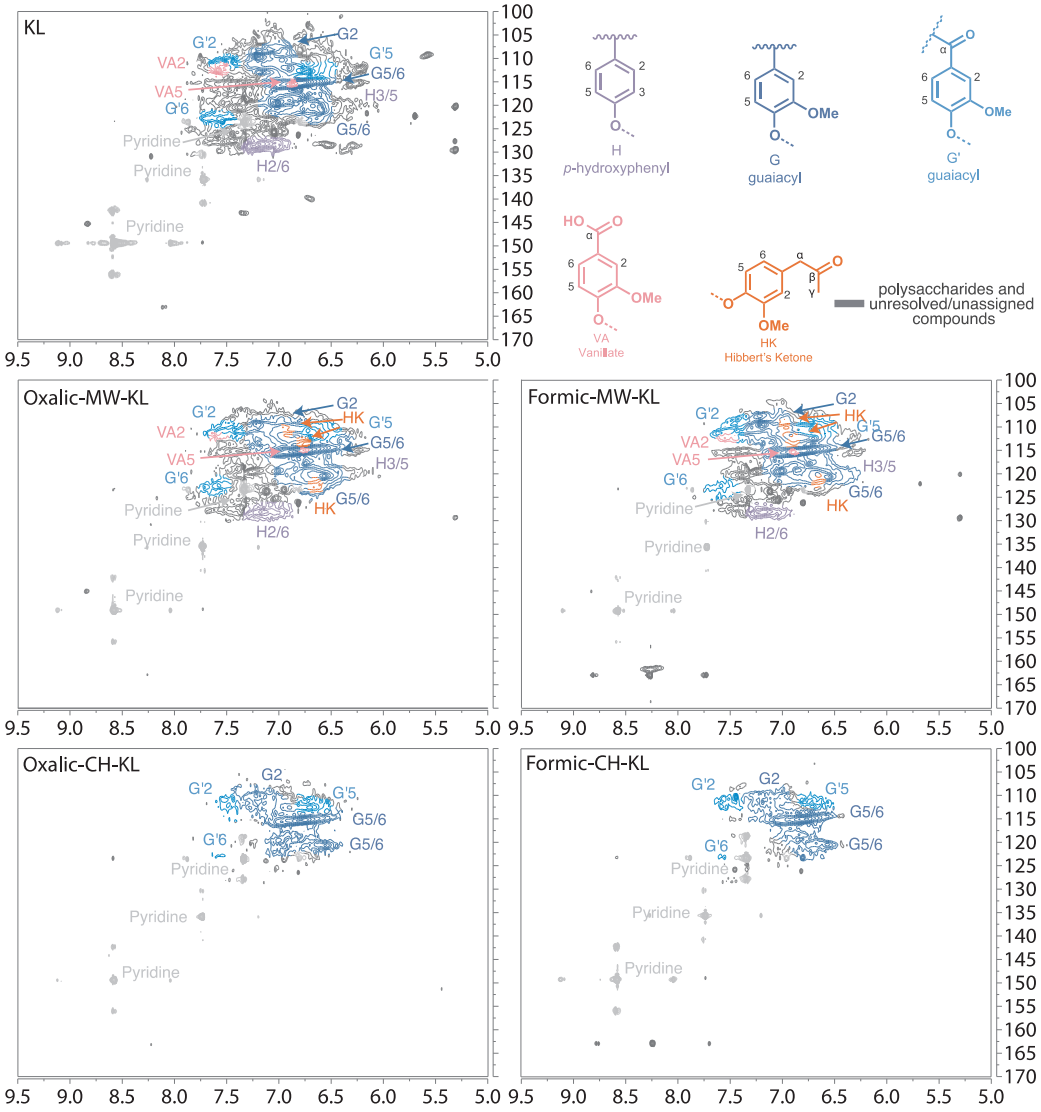

Fig. 7. HSQC NMR spectra of the aromatic region of kraft lignin before and after MW and CH treatment in DES.

prominent for all samples including native kraft lignin [23,47,48]. The cross-signals of the phenylcoumaran structures (B_α δ_C/δ_H 87/5.6, B_β δ_C/δ_H 53/3.6 and B_γ δ_C/δ_H 63/3.8, as seen in green) were observed for KL samples but disappeared for processed lignin samples. Pinoresinol substructures (C_α, δC/δH 85/4.7, C_β δC/δH 54/3.1, and C_γ δC/δH 71/3.8, 4.2, as seen in brown) were still present but had reduced in intensity for processed lignin samples. Integrations were not used for HSQC analysis of the aliphatic area due to the complete loss of *β-O-4* and *β-5* cross-peaks [23]. The most striking difference here was the formation of cross-peaks consistent with Hibbert's ketone (HK) in microwave treated lignin and the lack of HK in conventional treated lignin [11]. Note, while Oxalic-CH-KL appeared to show a peak consistent with HK_α, the absence of an HK_γ precludes this assignment as a Hibbert's Ketone. HK is typically seen when the *α-OH* in the *β-O-4* structure is dehydrated to an enol ether [11]. In the presence of an acid (and some water), the enol ether should cleave (hydrolyze) to make Hibbert's Ketone. The presence of cross-peaks consistent with HK suggests that this mechanism may be occurring during MW heating. The dominant peaks in the aromatic region of the kraft lignin were p-hydroxyphenyl (H), guaiacyl (G), guaiacyl (G′) and vanillate (VA) (Fig. 7). The signal intensity of the aromatic region of the CH samples was significantly less intense than that of the KL and MW samples. This is potentially due to decreased solubility due to the more condensed nature of the conventionally heated samples. Interestingly, in the aromatic region of the HSQC spectra, microwave treated samples displayed relatively little difference, from the original kraft lignin. HK cross-peaks are highlighted here to suggest where the cross-peaks would show up, however, they are, in general hidden beneath already present peaks from kraft lignin. The peak intensities decreased for p-hydroxyphenyl (H), guaiacyl (G) and, guaiacyl (G'), The cross-signals of xylans in benzyl ester structures β-dxylopyranoside, 3-*O*-acetyl-β-D-xylopyranoside and 2-*O*-acetyl-β-D-xylopyranoside (X2, X3, X4, X5) were detected in native kraft lignin [23], however these xylans were not visible for DES treated lignin samples, which may suggest the cleavage of primary linkages between xylans and lignin.

The molecular dynamic simulation results are discussed below. The tetramer molecules which were studied are shown in Fig. 8. The structure of the two G tetramers with all β-O-4 linkages and different chirality are shown in Fig. 8(a). Specifically, each β-O-4 linkage contains two chiral centers. The difference between the two tetramers was that the central linkage had either S,S chirality or R,S chirality. In addition, one G tetramer with β-O-4, β-5, β-O-4 linkages was also considered (see Fig. 8(b)). Bonds which have differences in lengths greater than their uncertainties with and without electric field are marked on the structures. Note that all differences are only on the order of 10^{-4} nm or smaller which is expected since forces due to the electric field are

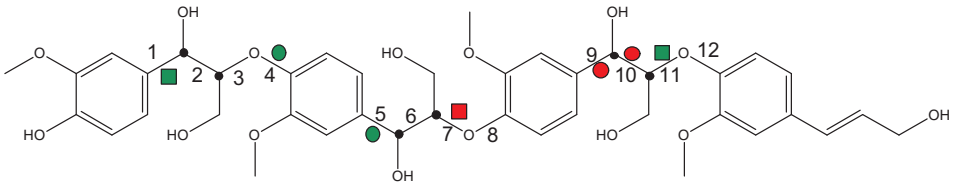

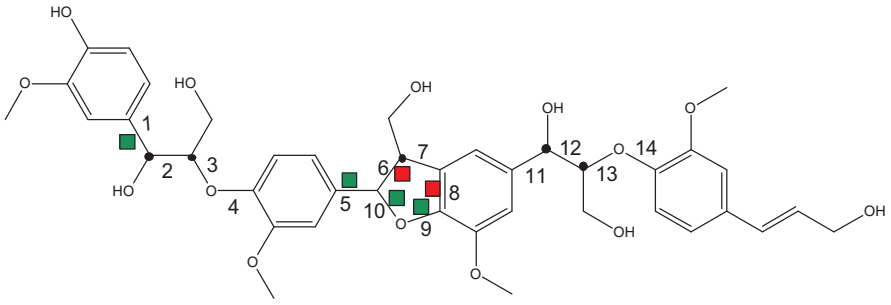

Fig. 8. Tetramers considered. Chiral centers are marked with a black dot. Bonds which were significantly longer with electric field are marked in red and bonds which were significantly shorter with electric field are marked in green. (a) All β-O-4 linkages. Isomers considered were R,R,S,S,R,S (bonds with significant changes marked with squares) or R,R,R,S,R,S (bonds with significant changes marked with circles) starting from the left. (b) β-O-4, β-5, β-O-4 linkages.

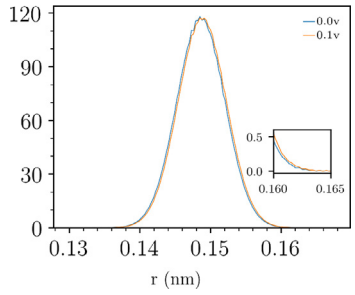

Fig. 9. Bond length probability density distributions for the all β-O-4 linkage R,R,S,S,R,S isomer bond 7 with E = 0.0 V/nm and E = 0.1 V/nm. The inset is the right tail.

small compared to thermal fluctuations. The bond with the lowest dissociation energy [49] in the β-O-4 linkages is the C_β-O bond which is bonds 3, 7, and 11 in Fig. 8(a) and bonds 3 and 13 in Fig. 8(b). Bond 7 in the all β-O-4 R,R,S,S,R,S isomer was significantly longer with electric field (Fig. 9), but none of the other C_β-O bond lengths were increased significantly by the electric field. Other bonds with increased lengths were bonds 9 and 10 in Fig. 8(a) for the R,R,R,S,R,S isomer, and bonds 6 and 8 Fig. 8(b) for the β-5 linkage. Bonds with decreased lengths were bonds 1 and 11 in Fig. 8(a) for the R,R,S,S,R,S isomer, bonds 4 and 5 in Fig. 8(a) for the R,R,R,S,R,S isomer, and bonds 1, 5, 9, and 10 in Fig. 8(b) for the β-5 linkage. Results for mean bond length differences and differences in probabilities of the bond lengths being greater than cutoff distances equal to the 99th percentiles in the zero field cases for all bonds are in Supplementary Information.

These results show that the electric field does increase some of the bond lengths including C_β-O in the β-O-4 linkage, but which bonds are affected seems to be a function of the overall conformation of the molecule which is a function of its stereochemistry. Changing one chiral center does not only change the bond length behavior for its linkage, but for the whole molecule. Based on these simulations it seems likely that some of the bonds in real lignin are stretched on average by the microwaves leading to an increased probability of breaking and therefore an increased rate of breakdown of the polymer.

4. Conclusions

The study shows that deep eutectic solvents are effective at selectively dissolving lignin during biomass fractionation. Microwave heating enhances this process through faster heating rates. Lignin depolymerization occurred during biomass fractionation. Oxalic acid and formic acid DES gave the highest lignin yield. NMR analysis showed that microwave heating was more effective in selective bond breakage during kraft lignin depolymerization. GPC analysis showed a relatively narrow molecular weight distribution in microwave treated lignin compared to conventional heating. MD simulations confirmed that certain lignin bonds are stretched under the microwave irradiation, which increases its probability of breaking. Based on this study, microwave heating can be effectively used for biomass deconstruction as well as lignin depolymerization using deep eutectic solvents, reducing processing time and increasing product selectivity.

Declaration of Competing Interest

The authors declare that they have no known competing financial interests or personal relationships that could have appeared to influence the work reported in this paper.

Acknowledgements

The authors would like to acknowledge LSU's Department of Biological and Agricultural Engineering, LSU's Center for Computation and Technology, LSU Agricultural Center, and USDA NIFA Hatch Program [project number LAB #94443], for their support of this project. Financial support was provided by US NSF OIA (award #1632854), and Louisiana Board of Regents (#Louisiana Board of Regents Support Fund (award #LEQSF(2015-17)-ENH-TR-01). Published with the approval of the Director of the Louisiana Agricultural Experiment Station as manuscript #2019-232- 33832.

Appendix A. Supplementary data

Supplementary data to this article can be found online at https://doi.org/10.1016/j.enconman.2019.06.070.

References

[1] Li M-F, Yu P, Li S-X, Wu X-F, Xiao X, Bian J. Sequential two-step fractionation of lignocellulose with formic acid organosolv followed by alkaline hydrogen peroxide under mild conditions to prepare easily saccharified cellulose and value-added lignin. Energy Convers Manage 2017;148:1426–37.
[2] Chen D, Gao A, Cen K, Zhang J, Cao X, Ma Z. Investigation of biomass torrefaction based on three major components: Hemicellulose, cellulose, and lignin. Energy Convers Manage 2018;169:228–37.
[3] Mottiar Y, Vanholme R, Boerjan W, Ralph J, Mansfield SD. Designer lignins: harnessing the plasticity of lignification. Curr Opin Biotechnol 2016;37:190–200.

[4] Ragauskas AJ, Beckham GT, Biddy MJ, Chandra R, Chen F, Davis MF, et al. Lignin valorization: improving lignin processing in the biorefinery. Science 2014;344(6185):1246843.

[5] Shen D, Zhao J, Xiao R. Catalytic transformation of lignin to aromatic hydrocarbons over solid-acid catalyst: Effect of lignin sources and catalyst species. Energy Convers Manage 2016;124:61–72.

[6] Gellerstedt G, Henriksson G. Lignins: major sources, structure and properties. In *Monomers, polymers and composites from renewable resources*. Elsevier; 2008. p. 201–24.

[7] Studer MH, DeMartini JD, Davis MF, Sykes RW, Davison B, Keller M, et al. Lignin content in natural Populus variants affects sugar release. Proc Natl Acad Sci 2011;108(15):6300–5.

[8] Ragauskas AJ, Beckham GT, Biddy MJ, Chandra R, Chen F, Davis MF, Davison BH, Dixon RA, Gilna P, Keller M, Langan P, Naskar AK, Saddler JN, Tschaplinski TJ, Tuskan GA, Wyman CE. Lignin valorization: improving lignin processing in the biorefinery. Science 2014;344(6185):1246843. https://doi.org/10.1126/science:1246843.

[9] Laskar DD, Yang B, Wang H, Lee J. Pathways for biomass-derived lignin to hydrocarbon fuels. Biofuels, Bioprod Biorefin 2013;7(5):602–26.

[10] Wang H-M, Wang B, Wen J-L, Wang S-F, Shi Q, Sun R-C. Green and efficient conversion strategy of Eucalyptus based on mechanochemical pretreatment. Energy Convers Manage 2018;175:112–20.

[11] Alvarez-Vasco C, Ma R, Quintero M, Guo M, Geleynse S, Ramasamy KK, et al. Unique low-molecular-weight lignin with high purity extracted from wood by deep eutectic solvents (DES): a source of lignin for valorization. Green Chem 2016;18(19):5133–41.

[12] Li C, Tanjore D, He W, Wong J, Gardner JL, Sale KL, et al. Scale-up and evaluation of high solid ionic liquid pretreatment and enzymatic hydrolysis of switchgrass. Biotechnol Biofuels 2013;6(1):154.

[13] Shi J, Gladden JM, Sathitsuksanoh N, Kambam P, Sandoval L, Mitra D, et al. One-pot ionic liquid pretreatment and saccharification of switchgrass. Green Chem 2013;15(9):2579–89.

[14] Datta S, Holmes B, Park JI, Chen Z, Dibble DC, Hadi M, et al. Ionic liquid tolerant hyperthermophilic cellulases for biomass pretreatment and hydrolysis. Green Chem 2010;12(2):338–45.

[15] Zhang Q, Vigier KDO, Royer S, Jérôme F. Deep eutectic solvents: syntheses, properties and applications. Chem Soc Rev 2012;41(21):7108–46.

[16] Abbott AP, Boothby D, Capper G, Davies DL, Rasheed RK. Deep eutectic solvents formed between choline chloride and carboxylic acids: versatile alternatives to ionic liquids. J Am Chem Soc 2004;126(29):9142–7.

[17] Bhatia SK, Joo H-S, Yang Y-H. Biowaste-to-bioenergy using biological methods – a mini-review. Energy Convers Manage 2018;177:640–60.

[18] Kandanelli R, Thulluri C, Mangala R, Rao PVC, Gandham S, Velankar HR. A novel ternary combination of deep eutectic solvent-alcohol (DES-OL) system for synergistic and efficient delignification of biomass. Bioresour Technol 2018;265:573–6.

[19] Lynam JG, Kumar N, Wong MJ. Deep eutectic solvents' ability to solubilize lignin, cellulose, and hemicellulose; thermal stability; and density. Bioresour Technol 2017;238:684–9.

[20] Chen Z, Wan C. Ultrafast fractionation of lignocellulosic biomass by microwave-assisted deep eutectic solvent pretreatment. Bioresour Technol 2018;250:532–7.

[21] Francisco M, van den Bruinhorst A, Kroon MC. Low-transition-temperature mixtures (LTTMs): a new generation of designer solvents. Angew Chem Int Ed 2013;52(11):3074–85.

[22] Tang X, Zuo M, Li Z, Liu H, Xiong C, Zeng X, et al. Green processing of lignocellulosic biomass and its derivatives in deep eutectic solvents. ChemSusChem 2017;10(13):2696–706.

[23] Liu Y, Chen W, Xia Q, Guo B, Wang Q, Liu S, et al. Efficient cleavage of lignin-carbohydrate complexes and ultrafast extraction of lignin oligomers from wood biomass by microwave-assisted treatment with deep eutectic solvent. ChemSusChem 2017;10(8):1692–700.

[24] Chen Z, Bai X, Wan C. High-solid lignocellulose processing enabled by natural deep eutectic solvent for lignin extraction and industrially relevant production of renewable chemicals. ACS Sustainable Chem Eng 2018;6(9):12205–16.

[25] Kappe CO. Microwave dielectric heating in synthetic organic chemistry. Chem Soc Rev 2008;37(6):1127–39.

[26] Tsegaye B, Balomajumder C, Roy P. Optimization of microwave and NaOH pretreatments of wheat straw for enhancing biofuel yield. Energy Convers Manage 2019;186:82–92.

[27] Aguilar-Reynosa A, Romaní A, Rodríguez-Jasso Ma, Aguilar R, Garrote CN, Ruiz G. Microwave heating processing as alternative of pretreatment in second-generation biorefinery: an overview. Energy Convers Manage 2017;136:50–65.

[28] Wei G, Liu Z, Zhang L, Li Z. Catalytic upgrading of Jatropha oil biodiesel by partial hydrogenation using Raney-Ni as catalyst under microwave heating. Energy Convers Manage 2018;163:208–18.

[29] de la Hoz A, Diaz-Ortiz A, Moreno A. Microwaves in organic synthesis. Thermal and non-thermal microwave effects. Chem Soc Rev 2005;34(2):164–78.

[30] Kumar AK, Parikh BS, Pravakar M. Natural deep eutectic solvent mediated pretreatment of rice straw: bioanalytical characterization of lignin extract and enzymatic hydrolysis of pretreated biomass residue. Environ Sci Pollut Res 2016;23(10):9265–75.

[31] Sun N, Rahman M, Qin Y, Maxim ML, Rodríguez H, Rogers RD. Complete dissolution and partial delignification of wood in the ionic liquid 1-ethyl-3-methylimidazolium acetate. Green Chem 2009;11(5):646–55.

[32] Guerra A, Lucia LA, Argyropoulos DS. Isolation and characterization of lignins from Eucalyptus grandis Hill ex Maiden and Eucalyptus globulus Labill. by enzymatic mild acidolysis (EMAL). Holzforschung 2008;62(1):24–30.

[33] Abraham MJ, Murtola T, Schulz R, Páll S, Smith JC, Hess B, et al. GROMACS: High performance molecular simulations through multi-level parallelism from laptops to supercomputers. SoftwareX 2015;1:19–25.

[34] Vanommeslaeghe K, Hatcher E, Acharya C, Kundu S, Zhong S, Shim J, et al. CHARMM general force field: A force field for drug-like molecules compatible with the CHARMM all-atom additive biological force fields. J Comput Chem 2010;31(4):671–90.

[35] Zoete V, Cuendet MA, Grosdidier A, Michielin O. SwissParam: a fast force field generation tool for small organic molecules. J Comput Chem 2011;32(11):2359–68.

[36] Vermaas JV, Dellon LD, Broadbelt LJ, Beckham GT, Crowley MF. Automated Transformation of Lignin Topologies into Atomic Structures with LigninBuilder. ACS Sustainable Chem Eng 2018.

[37] Martínez L, Andrade R, Birgin EG, Martínez JM. PACKMOL: a package for building initial configurations for molecular dynamics simulations. J Comput Chem 2009;30(13):2157–64.

[38] Bplincs H. A parallel linear constraint solver for molecular simulation. J Chem Theory Comput 2008;4:116–22.

[39] Essmann U, Perera L, Berkowitz ML, Darden T, Lee H, Pedersen LG. A smooth particle mesh Ewald method. J Chem Phys 1995;103(19):8577–93.

[40] Bussi G, Donadio D, Parrinello M. Canonical sampling through velocity rescaling. J Chem Phys 2007;126(1). 014101.

[41] Muley PD, Boldor D. Investigation of microwave dielectric properties of biodiesel components. Bioresour Technol 2013;127:165–74.

[42] Ang A, Ashaari Z, Bakar ES, Ibrahim NA. Characterisation of sequential solvent fractionation and base-catalysed depolymerisation of treated alkali lignin. BioResources 2015;10(3):4137–51.

[43] Yoo CG, Li M, Meng X, Pu Y, Ragauskas AJ. Effects of organosolv and ammonia pretreatments on lignin properties and its inhibition for enzymatic hydrolysis. Green Chem 2017;19(8):2006–16.

[44] Sirviö JA, Visanko M, Liimatainen H. Deep eutectic solvent system based on choline chloride-urea as a pre-treatment for nanofibrillation of wood cellulose. Green Chem 2015;17(6):3401–6.

[45] Casas A, Alonso MV, Oliet M, Rojo E, Rodríguez F. FTIR analysis of lignin regenerated from Pinus radiata and Eucalyptus globulus woods dissolved in imidazolium-based ionic liquids. J Chem Technol Biotechnol 2012;87(4):472–80.

[46] Tabasso S, Grillo G, Carnaroglio D, Calcio Gaudino E, Cravotto G. Microwave-assisted γ-valerolactone production for biomass lignin extraction: a cascade protocol. Molecules 2016;21(4):413.

[47] Jiang B, Zhang Y, Guo T, Zhao H, Jin Y. Structural characterization of lignin and lignin-carbohydrate complex (LCC) from ginkgo shells (Ginkgo biloba L.) by comprehensive nmr spectroscopy. Polymers 2018;10(7):736.

[48] Lancefield CS, Ojo OS, Tran F, Westwood NJ. Isolation of functionalized phenolic monomers through selective oxidation and C-O bond cleavage of the β-O-4 linkages in lignin. Angew Chem 2015;127(1):260–4.

[49] Huang J-B, Wu S-B, Cheng H, Ming L, LIANG J-J, Hong T. Theoretical study of bond dissociation energies for lignin model compounds. J Fuel Chem Technol 2015;43(4):429–36.